



## Article

# GPTFF: A high-accuracy out-of-the-box universal AI force field for arbitrary inorganic materials

Fankai Xie <sup>a,b</sup>, Tenglong Lu <sup>a,b</sup>, Sheng Meng <sup>a,b,\*</sup>, Miao Liu <sup>a,b,\*</sup>

<sup>a</sup> Beijing National Laboratory for Condensed Matter Physics, Institute of Physics, Chinese Academy of Sciences, Beijing 100190, China

<sup>b</sup> Songshan Lake Materials Laboratory, Dongguan 523808, China

## ARTICLE INFO

## Article history:

Received 20 June 2024

Received in revised form 5 August 2024

Accepted 20 August 2024

Available online 1 September 2024

## Keywords:

Data science

Molecular dynamics

Graph neural network

Universal force field

## ABSTRACT

This study introduces a novel artificial intelligence (AI) force field, namely a graph-based pre-trained transformer force field (GPTFF), which can simulate arbitrary inorganic systems with good precision and generalizability. Harnessing a large trove of the data and the attention mechanism of transformer algorithms, the model can accurately predict energy, atomic force, and stress with mean absolute error (MAE) values of 32 meV/atom, 71 meV/Å, and 0.365 GPa, respectively. The dataset used to train the model includes 37.8 million single-point energies, 11.7 billion force pairs, and 340.2 million stresses. We also demonstrated that the GPTFF can be universally used to simulate various physical systems, such as crystal structure optimization, phase transition simulations, and mass transport. The model is publicly released with this paper, enabling anyone to use it immediately without needing to train it.

© 2024 The Authors. Published by Elsevier B.V. and Science China Press. This is an open access article under the CC BY license (<http://creativecommons.org/licenses/by/4.0/>).

## 1. Introduction

Molecular dynamics (MD) solves Newton's equations of motion to monitor particle positions and velocities as a function of time, and can simulate phenomena such as protein folding, chemical reactions, and phase transitions, offering insights into the behaviors of materials from the atomistic level [1–6]. The method is limited primarily to the accuracy of the force fields, which represent how the atoms interact with each other at the microscopic scale. Improving the force fields is a central topic for the MD community. The MD method is presently undergoing a drastic transformation when artificial intelligence (AI) and high-throughput computation are introduced: the AI allows the force field to have several magnitudes more parameters to outperform the traditional analytic force field function form; the high-throughput computation creates the dataset for AI model training process, level-up the accuracy of the force fields [7,8]. Recently, the raising of AI force fields has improved the accuracy and applicability of force fields notably, propelling MD to a stage where simulations can be accelerated by up to  $10^6$  times compared to the efficiency of density functional theory (DFT) [9] without sacrificing accuracy too much [10–13]. The path forward for the MD method is clear – the key is to develop a powerful interatomic force field based on AI and data.

In the past, significant progress has been achieved in developing the AI force field, which can be divided into three stages. At the early stage, people focused on creating effective mathematical algorithms and descriptors to capture the key physics of interatomic interactions by working with a small dataset. For instance, the Smooth Overlap of Atomic Positions (SOAP) descriptor-based Gaussian approximation potential (GAP) [10,14] is of this kind, and there are many successors such as DeepMD [11], SNAP [15], NNP [12,13], and so on [16–19]. Subsequently, the emergence of neural networks and the expansion of available datasets propelled the AI force field to an elevated level. This advancement involved an increase in the number of parameters and data, leading to substantial improvements in model accuracy without requiring explicit descriptors. Examples of this stage include MegNet [20], DimeNet [21], SchNet [22], CGCNN [23], and ALIGNN [24]. More recently, models for atomistic materials science have progressed to a universal force field stage, necessitating the incorporation of a significant trove of data from both equilibrium and nonequilibrium states and an efficient training process. The obtained force field at this stage, such as M3GNet [25], CHGNet [26], PFP [27], and ALIGNN-FF [28], can be universally applied to nearly any close-to-equilibrium system.

As indicated by several existing pieces of literature, the progress of the AI force field is predominantly driven by advancements in data. Previously, Liang et al. [29] showcased that model accuracy increases marginally with the growth of data points, following a power law, meaning that increasing the size of the dataset by

\* Corresponding authors.

E-mail addresses: [smeng@iphy.ac.cn](mailto:smeng@iphy.ac.cn) (S. Meng), [mliu@iphy.ac.cn](mailto:mliu@iphy.ac.cn) (M. Liu).

one magnitude can improve the model accuracy twice (reduce to half of the mean average error). Deepmind's GNoME project [30] also supports this observation, suggesting that model improvement can be achievable through the inclusion of more data. On the other hand, the quality of data is crucial, but it is usually challenging to measure and benchmark the quality of the dataset quantitatively. The Materials Project [31], while not the largest computational DFT dataset, is highly valued for its superior data quality compared to numerous other available datasets [20,23,24], including some larger open-source alternatives [32]. Meanwhile, the AI algorithm itself is rapidly evolving in tandem with the recent advances in vision and language models [33,34]. Nowadays the algorithm developed for fundamental models can easily incorporate billions, if not trillions, of parameters [35]. This suggests that the AI force field, which usually has less than 1 million parameters, can be further improved if a sufficiently large, good-quality dataset can be obtained.

In this study, we would like to announce a new AI force field, namely graph-based pre-trained transformer force field (GPTFF), aiming to showcase the effectiveness of incorporating a large dataset, encompassing 37.8 million energies, 11.7 billion force pairs, and 340.2 million stresses, and beneficial of leveraging the attention mechanism inherent in transformer algorithms [36]. Through this approach, we have successfully developed a pre-trained transformer model capable of accurately predicting the energy, atomic forces, and stress of any given materials system, achieving the mean absolute error (MAE) values of 32 meV/atom, 71 meV/Å, and 0.365 GPa for energies, forces, and stress, respectively. Compared to the existing models, GPTFF can achieve better generalization. Furthermore, we have demonstrated its capacity for solving various physical science problems, such as optimizing structures of arbitrary compounds, simulating phase transition of a metal system under external strain, and investigating mass transportation phenomena in ionic compounds.

## 2. Methods

### 2.1. Model architecture

For the model construction, we employ graph neural networks (GNNs) [37–39] to represent crystal structures, as illustrated in Fig. 1. Like many pioneer force fields that require the construction of atomic coordinate descriptors to ensure rotational, translational, and permutation symmetries [10,11,15], using GNNs to represent crystal structures can easily satisfy these symmetry relationships. Each atom is projected into a high-dimensional space according to its element type and is represented in the form of an embedding vector. The geometric structure of each atom's local environment, such as the bond lengths between atoms, is represented by the edges in the GNN, forming an edge vector. The edge vector is represented by concatenating the node vectors representing the two atoms and the vector of information about the distance between them.

Additionally, we incorporate bond angle information related to three-body interactions into the model, achieved by concatenating the node and edge vectors of the atoms forming the bond angle. This allows the model to further learn the interaction relationships between different atomic nodes and edge vectors, thereby improving the model's predictive power significantly. During the high-dimensional representation process of the bond angle, we directly consider the neural network as a scalar function, thereby mapping the cosine value of the bond angle from one dimension to high dimensions.

In the model prediction and inference process, the vector representation within the atomic cutoff radius is predicted by the GNN into the form of atomic energy, and the sum of the atomic energies finally yields the total energy of the system. For the calculation of atomic forces, we use the method of automatic differentiation [40]. The force on an atom can be obtained from the negative gradient of

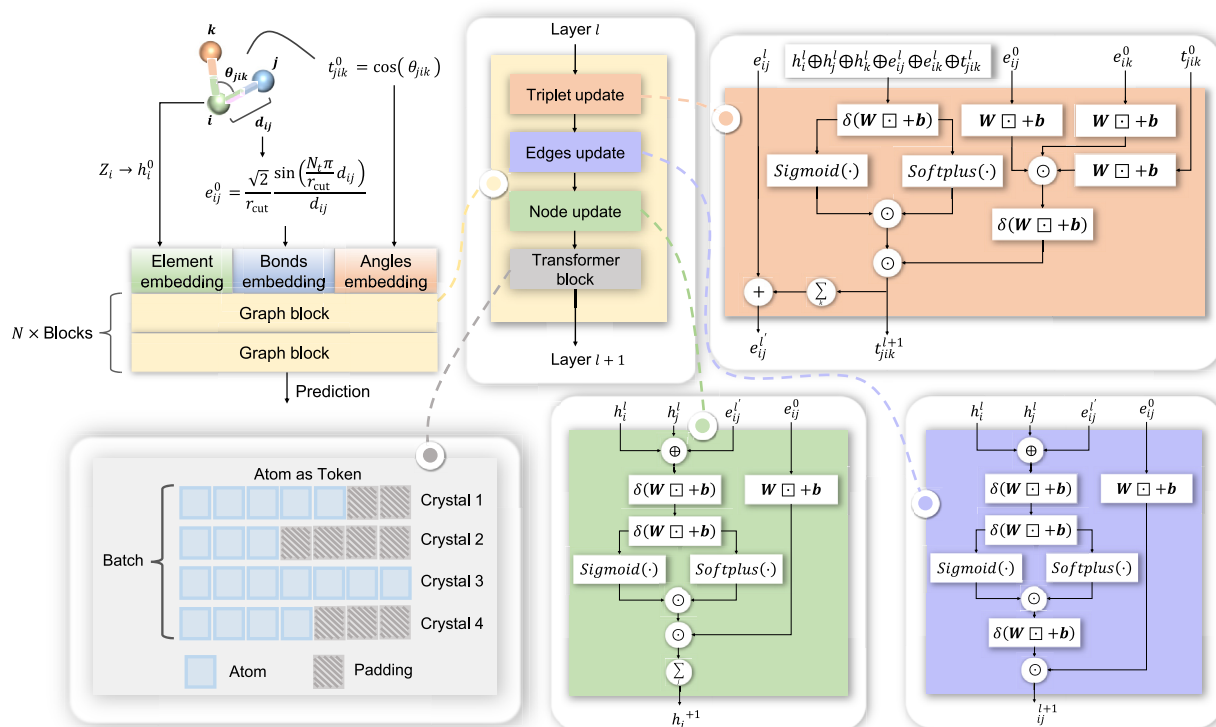


Fig. 1. Schematic of the model architecture. Information such as element, bond, angles and transformer are represented and updated in the graph block.

the total energy  $E$  with respect to the atomic coordinates, i.e.,  $\vec{F}_i = \frac{\partial E}{\partial \vec{x}_i}$ . The expression for stress calculation is:  $\vec{\sigma} = \frac{1}{V} \frac{\partial E}{\partial \vec{S}}$ , where

$V$  represents the volume of the system, and  $\vec{S}$  represents the strain of the system.

## 2.2. Dataset

The training dataset is provided by [Atomly.net](#) team, which includes the trajectory of structural optimization of 2,234,767 crystal structures using DFT. All the calculations are conducted utilizing the consistent calculation parameter to yield a dataset with good quality, e.g., GGA-PBE [41] is selected as the pseudopotential, the energy cutoff is 520 eV, and the 5.4 version of the POTCARs as implemented in the VASP code [42–45] is employed for all the calculations.

Overall, the dataset contains 37.8 million single-point energies, 11.7 billion atomistic force vectors, and 340.2 million stresses. Fig. 2a displays the statistics of the chance of the appearance of each element, and the chance of coappearance of two elements. Within the dataset, there are 349,043 single-point energies from the equilibrium state, and 37.4 million single-point energies from the nonequilibrium states, roughly 27.6 times larger than the MPtrj dataset [26]. The larger circle size in Fig. 2 denotes the higher frequency of appearance of the given element. The shade of the strings represents the likelihood they coexist in a single compound. Fig. 2a demonstrates that the dataset has an evenly distributed sampling of the entire phase space, covering a large and less biased structural space and chemical space.

## 2.3. Training process

The dataset was divided into training, validation, and test sets. In detail, as the dataset is gigantic, we randomly pick up 100,000

data points for validation and test sets separately, for faster validation. It is ensured that the crystal structures in the test set never co-appear in the training and validation sets to yield a valid model. We do not truncate or remove any data points in our dataset to ensure that the model has a good generalization. The AdamW [46] optimization is employed in our model, and a sampling learning method is adopted, where each epoch randomly samples about 1 million data from the training set for model training, with a total of 500 epochs.

Given the inherent limitations of GNNs, there is a saturation point at which increases in model depth and parameters fail to further enhance model performance [47]. To address this issue, we have incorporated Transformer [36] modules into our model. This integration serves to boost the number of parameters, enabling the model to learn a greater amount of latent information within the data. The model currently has 502,465 parameters and can be easily scaled to a larger model with more parameters, such as more than 1 million parameters. Transformers demand a relatively small learning rate during the training process to ensure model stability [48]. Consequently, we adopted an initial learning rate of  $2 \times 10^{-4}$  in our training process, which gradually decayed to  $5 \times 10^{-6}$  toward the end of the training. This strategy allows for a more controlled and stable training process, minimizing the risk of over-shooting the optimal solution and ensuring a robust and reliable model performance.

## 3. Results and discussion

### 3.1. Model performance

The GPTFF can accurately predict the energies, forces, and stress for any atomistic configuration, and hence can serve as a valid universal force field. In Fig. 3a–c, it is evident that GPTFF demonstrates an energy error as low as 32 meV/atom, force error of 71 meV/Å,

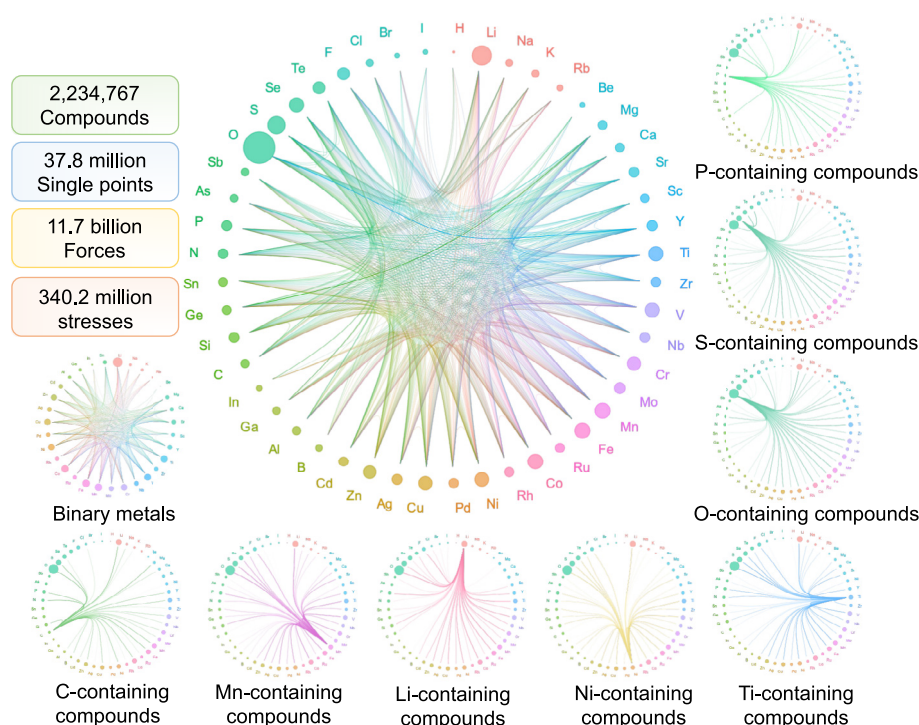


**Fig. 2.** Element and training data distribution in atomly database. The training data contains 2,234,767 compounds which generated about 37.8 million single points during structure optimization via DFT calculation.

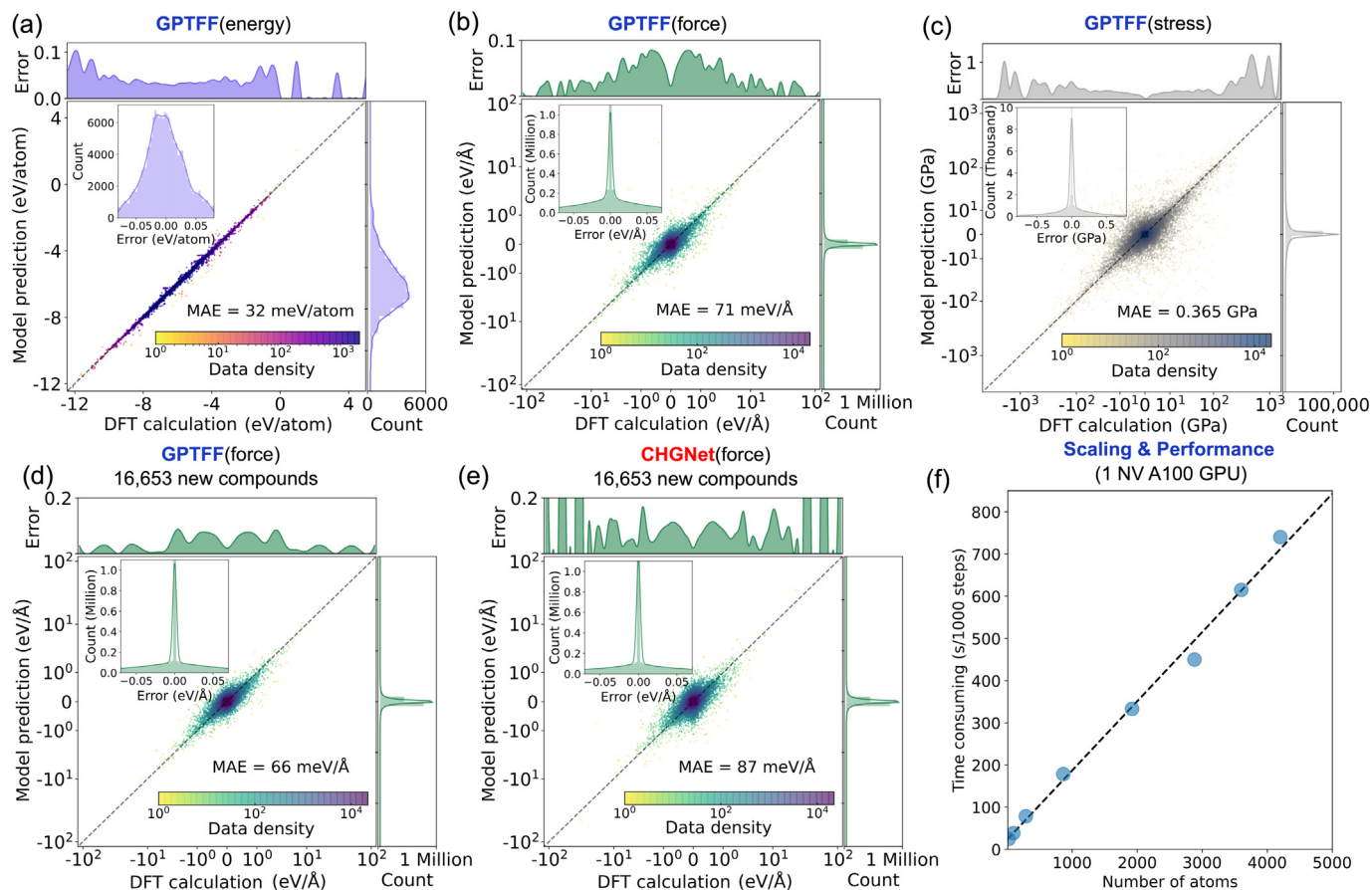


**Fig. 3.** (a–c) The evaluation of MAE results and data distribution of universal force field model on energy, force, and stress regression targets in the test dataset. (d, e) The model performance comparison of our model (d) vs. CHGNet (e). The validation set consists of new structures that do not appear in either the Materials Project or the GPTFF training set. The shades of the colors indicate the density of the data points. (f) The efficiency and scalability of the model.

and system stress error of 0.365 GPa on the test dataset. These results outperform both the M3GNet (MAE=35 meV/atom) and CHGNet (MAE=33 meV/atom, without magmom) due to our AI force field being constructed from a substantially large dataset, enhancing the model's overall generalizability.

For a testing purpose, we conducted additional performance tests on our model and CHGNet for comparison, utilizing a small testing dataset of 16,653 structures, in which all the compounds are new and do not exist in either the Materials Project or our training dataset. As depicted in Fig. 3d, e, in this test, the accuracy of CHGNet drops to 87 meV/Å for atomic forces, while our model achieved a higher prediction accuracy of 66 meV/Å.

As shown in Fig. 3f, the GPTFF model demonstrates impressive efficiency and scalability. The results indicate that the model can perform inference for 1000 steps on a system with 3000 atoms in just 500 s using a single Nvidia A100 GPU. Furthermore, the model's performance scales linearly, meaning that simulating 10,000 atoms for 50,000 steps would only require 1 day, or optimizing the structure of 100 atoms (typically needing 200 steps) would take just 3 s. Besides, running the GPTFF model on a CPU typically slows down the speed by two orders of magnitude compared to using a GPU, depending on the specific CPU hardware.

### 3.2. Application on structural optimization

One of the fundamental applications of a universal force field is its ability to quickly optimize any given crystal structure, making it suitable for rapid screening and relaxing unknown structures. It is

common practice to create new structures by element substitution, and element substitution will introduce strain in the system as the size of different atom species is not the same, therefore the newly generated structures are not in an equilibrium state, and a structure optimization process is required at this point. GPTFF can be employed to quickly optimize these structures. To demonstrate it, we conducted the calculation of the equation of state on the 39 structures using both the DFT and GPTFF. Those 39 compounds cover both ionic compounds and alloys. As shown in Fig. 4, the GPTFF can accurately calculate the equation of state of those systems and find the correct equilibrium volume ( $R^2 = 0.996$ ). It implies that the GPTFF has good precision, and the model can be universally applied to various systems to predict the equilibrium structures and energies.

### 3.3. Application on MD simulation

We also conducted tests using the GPTFF to run MD simulations for both metal and ionic compounds. Previously, it was not feasible for empirical MD to easily and accurately simulate ionic compounds as there is no accurate out-of-the-box force field for this type of compound [26]. For the metal system, we examined the phase transitions in titanium (Ti) from HCP to FCC due to stretching along  $[10\bar{1}0]$  direction; while for ionic compounds, we calculated the ionic conductivity of the Li cations in  $\text{Li}_3\text{YCl}_6$  system, which is a useful solid-state electrolyte material for lithium ionic batteries.

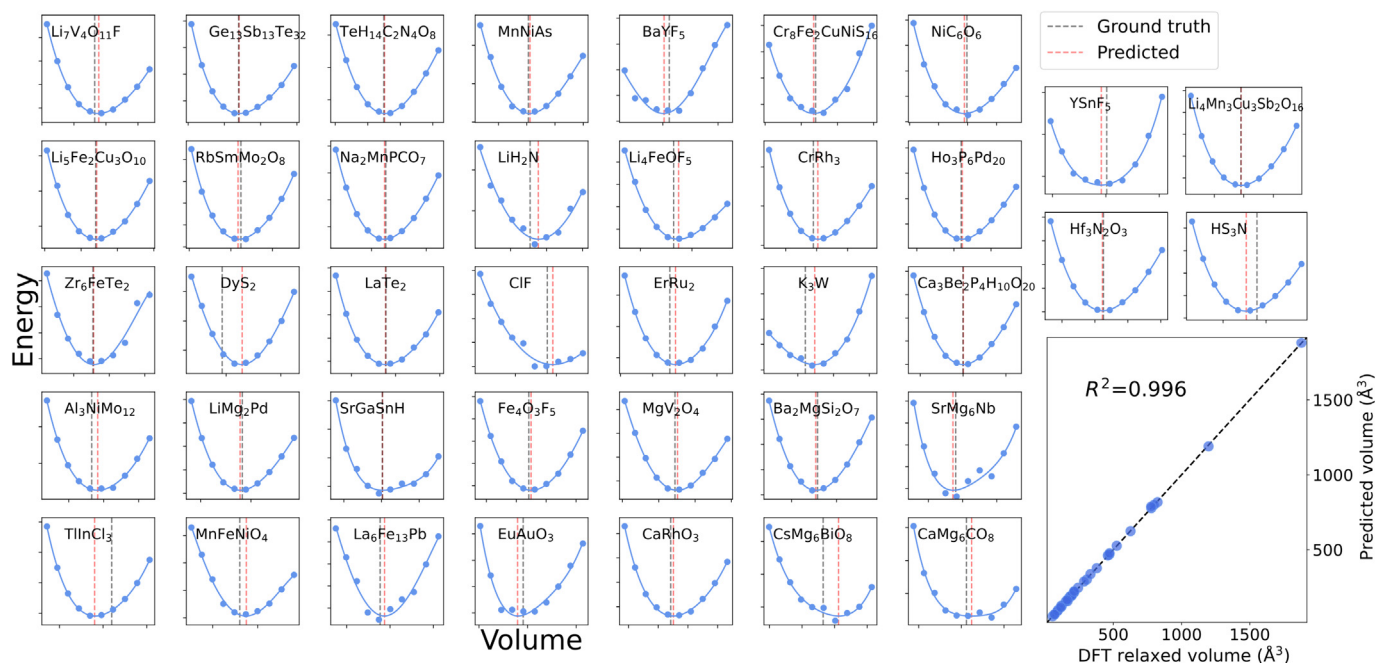


**Fig. 4.** The equation of state results predicted by our universal force field. The model optimizes the structure from initial unrelaxed structure. The black dashed line represents the final optimized result from DFT, while the red dashed line represents the volume at the equilibrium position after optimization by the force field model.

### 3.3.1. Force field for Titanium (Ti)

There is existing experimental literature indicating that for the HCP-stacked titanium system, if a tensile strain is applied in the  $[10\bar{1}0]$  crystal direction, the  $(10\bar{1}0)$  crystal plane slips, thereby generating a  $\frac{1}{6} < 1\bar{2}10 >$  Shockley partial dislocation [49,50]. The generation of this dislocation exactly transforms the HCP-stacked titanium system into an FCC-stacked titanium system. Accurately capturing such HCP-to-FCC phase transition requires a high-precision force field. Previously, the empirical embedded atom potential usually had an issue distinguishing the energies of HCP and FCC, as both structures are close-packed and have the same first-shell coordination numbers. Generally, the empirical embedded atom potential has difficulties in distinguishing two phases, leading to the development of several modified versions of embedded atom potentials to mitigate this issue [51,52]. However, none of them can reach an accuracy close to that of DFT and capture the HCP-to-FCC phase transition energies correctly.

As shown in Fig. 5, by utilizing the GPTFF, the HCP-to-FCC phase transition can be very well simulated in MD runs. In the MD simulation, the system has 1008 atoms. The NVT ensemble is selected at a low temperature of  $\sim 100$  K, to avoid thermodynamic disturbances as higher temperatures would vibrate the atoms to blur the peaks on the XRD pattern. Fig. 5c shows the snapshot of the crystal structures and XRD peaks during the entire HCP-to-FCC phase transition simulation process. As the MD progresses, an FCC phase peak starts to appear at about  $38^\circ$  on the XRD spectrum, indicating the occurrence of the phase change, which can also be seen on the atomic structures, in which the red and green regions represent the HCP and FCC stacking respectively.

### 3.3.2. Force field for $\text{Li}_3\text{YCl}_6$

Fast lithium cation transportation is crucial for solid lithium electrolytes in lithium-ion batteries [53]. A typical characteristic of superionic conductors is that within a large temperature range, the diffusion coefficient may follow different Arrhenius equations at different temperature regions as the high temperature opens up new diffusion channels, dividing the Arrhenius plots into two

zones. To verify the accuracy of the universal force field in ionic systems, we used the force field model to perform molecular dynamics simulations on the  $\text{Li}_3\text{YCl}_6$  system and calculated the ionic conductivity at different temperatures from 300 to 700 K (Fig. 6). Considering the volume expansion effect as well as the

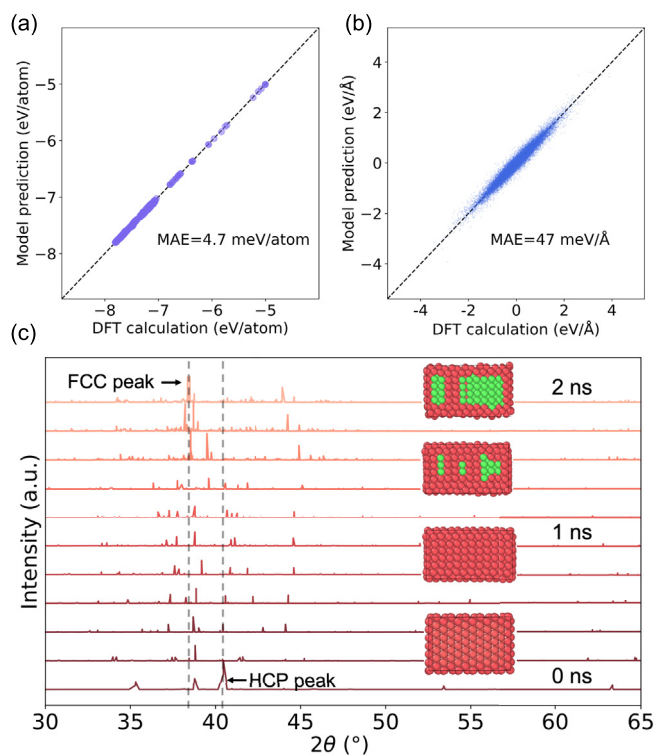


**Fig. 5.** (a, b) Finetuning results of energy and forces. (c) XRD results during MD simulation. With increasing of strain in  $[10\bar{1}0]$  direction, HCP→FCC phase transition occurs in the titanium system.

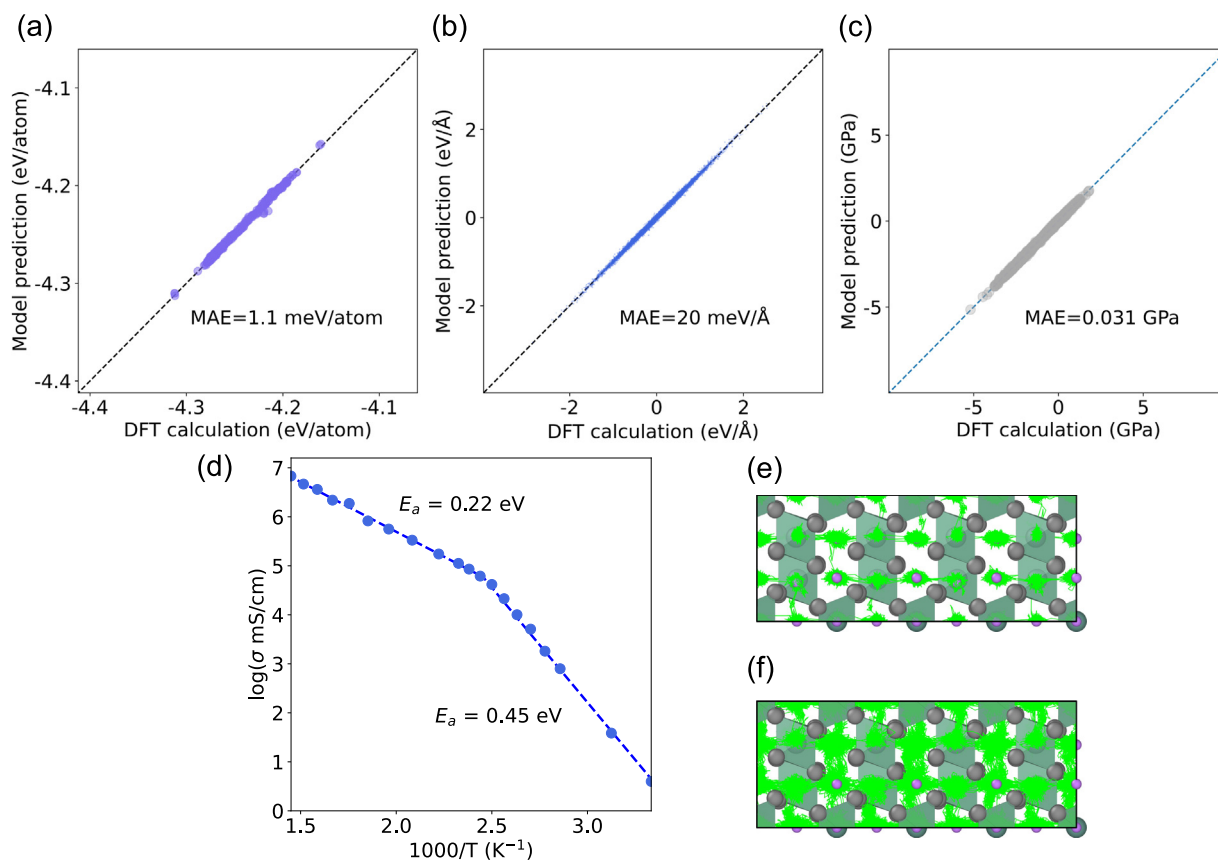


**Fig. 6.** (a–c) Finetuning results of energy, force and stress. (d) The relationship between temperature and ionic conductivity of  $\text{Li}_3\text{YCl}_6$ . (e, f) Trajectory of lithium ions at 300 and 500 K.

possible phase transitioning brought by temperature, we used the NPT ensemble in the simulation. Since the van der Waals interactions are important, especially in the  $\text{Li}_3\text{YCl}_6$  system [54], we used the optB88 [55] corrected DFT to accurately calculate the structural data of a small amount of  $\text{Li}_3\text{YCl}_6$  at different temperatures to obtain a dataset of about 2000 snapshots, and then finetuned the GPTFF. By adding a small amount of data, the pre-trained model can be further finetuned to a much more accurate form of a specific system, which is  $\text{Li}_3\text{YCl}_6$  in this case.

Then, we performed molecular dynamics simulations utilizing the finetuned model. Fig. 6d shows the ionic conductivity at different temperatures. The ionic conductivity at 300 K calculated using the GPTFF, which is 0.6 mS/cm, is in good agreement with the experimental observation, which is 0.51 mS/cm [56]. Fig. 6e, f shows that the lithium diffusion channel below transition temperature is mainly concentrated in one dimension. With the temperature going up above the transition point, a new diffusion channel of lithium cations opens up in all three dimensions. The force field model accurately predicts a superionic transition temperature of 425 K. Under the temperature range of 230–360 K, the activation energy as predicted from the model is 0.45 eV, in line with the experimental observations, which is 0.40 eV [56]. The result is also in good agreement with another AI force field [57]. These results reflect the high accuracy of the GPTFF for the calculation of the ionic compounds.

The emergence of the universal AI force field has opened a new avenue for theoretical materials science and chemistry. These models facilitate rapid, high-precision theoretical simulations and property predictions for arbitrary systems, reshaping the methodologies that were built on top of traditional DFT computations and empirical force fields. Harnessing the advance of the AI

force field, it becomes feasible to conduct high-efficiency and high-accuracy MD calculations.

### 3.4. Perspectives

In this work, we have developed the GPTFF and demonstrated its accuracy and convenience in property prediction and atomic scale simulation. Leveraging the dataset that covers large chemical and structural phases of inorganic compounds, the GPTFF model endows superior generalization capabilities. In principle, a critical determinant in the training process is not solely the model architecture but more importantly, the quality of the data employed, suggesting that the dataset is the fundamental of this type of research, hence credit should be given to people who build up the dataset.

The GPTFF employs a unique network architecture that ensures the model is lightweight yet powerful, enabling fast and accurate inference even on personal devices like laptops. Previously, running MD simulations for ionic compounds was a challenging task. However, GPTFF instantly provides a solution, as it is a universal machine learning potential that can simulate nearly every inorganic compound.

Currently, the supervision labels for GPTFF include energy, atomic forces, and system stress, which indeed utilize only a small amount of information generated by the DFT runs, whereas the information about electron-related properties is mostly ignored at the current level of models. In the forthcoming efforts, the community may aim to enhance the robustness of atomistic AI models by incorporating more data and labels. CHGNet has demonstrated that plugging the magnetic moments into the model can level up the predictive power, and this would be a useful strategy. In the

future, we plan to refine the self-attention mechanism within the transformer architecture to include more geometric information and to increase the model parameters. These would progressively make GPTFF more powerful. More rigorous tests will be performed [58,59], and the results will be published in separate papers in the future.

#### 4. Conclusion

The physical science community has a keen interest in developing a universal force field that possesses outstanding accuracy and broad applicability across all compounds. Our paper introduces an innovative artificial intelligence universal force field named the GPTFF, which establishes a new standard for simulating inorganic systems with unprecedented precision and adaptability, enabling the direct simulation of arbitrary inorganic materials. By harnessing the power of GPTFF, researchers can accurately simulate the behavior of a wide range of inorganic compounds, approaching the accuracy of density functional theory, while achieving speeds similar to those of classical molecular dynamics, speeding the simulation speed by  $\sim 1$  million times compared to DFT. It is demonstrated that GPTFF can optimize arbitrary crystal structures rapidly and can be used for large-scale atomic simulation, which enables further exploration of larger materials phase spaces for speeding up the discovery of new materials. This universal force field has the potential to significantly advance the field of physical science to new heights.

#### Conflict of interest

The authors declare that they have no conflict of interest.

#### Acknowledgments

This research was supported by the National Natural Science Foundation of China (12025407 and 11934003), Chinese Academy of Sciences (CAS-WX2023SF-0101, XDB33020000, XDB33030100), and the National Key R&D Program of China (2021YFA0718700, 2021YFA1400200). The computational resource is provided by the Songshan Lake Materials laboratory.

#### Author contributions

Miao Liu and Sheng Meng conceived and guided the development of this work. Fankai Xie carried out code development, model training, testing and application to scientific problems. Tenglong Lu provided contributions to  $\text{Li}_3\text{YCl}_6$  application. Fankai Xie prepared the first draft. Miao Liu and Sheng Meng reviewed the draft and provided modifications. Miao Liu supervised the whole study. All authors discussed and commented on the manuscript.

#### Data availability

The GPTFF, which is an open-source software under the GPLv3 License, can be downloaded from <https://github.com/atomly-materials-research-lab/GPTFF>. The package includes both the source code and the model parameters, allowing anyone to directly download and run the AI model in an out-of-the-box manner.

#### References

- [1] Hansson T, Oostenbrink C, van Gunsteren W. Molecular dynamics simulations. *Curr Opin Struct Biol* 2002;12:190–6.
- [2] Hollingsworth SA, Dror RO. Molecular dynamics simulation for all. *Neuron* 2018;99:1129–43.
- [3] Hospital A, Goñi JR, Orozco M, et al. Molecular dynamics simulations: Advances and applications. *Adv Appl Bioinf Chem* 2015;8:37–47.
- [4] Durrant JD, McCammon JA. Molecular dynamics simulations and drug discovery. *BMC Biol* 2011;9:71.
- [5] Rapaport DC. The art of molecular dynamics simulation. Cambridge: Cambridge University Press; 2004.
- [6] Binder K, Horbach J, Kob W, et al. Molecular dynamics simulations. *J Phys: Condens Matter* 2004;16:S429.
- [7] Unke OT, Chmiela S, Sauceda HE, et al. Machine learning force fields. *Chem Rev* 2021;121:10142–86.
- [8] Poltavsky I, Tkatchenko A. Machine learning force fields: Recent advances and remaining challenges. *J Phys Chem Lett* 2021;12:6551–64.
- [9] Payne MC, Teter MP, Allan DC, et al. Iterative minimization techniques for ab initio total-energy calculations: Molecular dynamics and conjugate gradients. *Rev Mod Phys* 1992;64:1045–97.
- [10] Bartók AP, Payne MC, Kondor R, et al. Gaussian approximation potentials: The accuracy of quantum mechanics, without the electrons. *Phys Rev Lett* 2010;104:136403.
- [11] Zhang L, Han J, Wang H, et al. Deep potential molecular dynamics: A scalable model with the accuracy of quantum mechanics. *Phys Rev Lett* 2018;120:143001.
- [12] Behler J, Parrinello M. Generalized neural-network representation of high-dimensional potential-energy surfaces. *Phys Rev Lett* 2007;98:146401.
- [13] Behler J. Atom-centered symmetry functions for constructing high-dimensional neural network potentials. *J Chem Phys* 2011;134:074106.
- [14] Bartók AP, Kondor R, Csányi G. Erratum: On representing chemical environments [Phys. Rev. B 87, 184115 (2013)]. *Phys Rev B* 2017, 96: 019902.
- [15] Thompson AP, Swiler LP, Trott CR, et al. Spectral neighbor analysis method for automated generation of quantum-accurate interatomic potentials. *J Comput Phys* 2015;285:316–30.
- [16] Shapeev AV. Moment tensor potentials: A class of systematically improvable interatomic potentials. *Multiscale Model Simul* 2016;14:1153–73.
- [17] Novikov IS, Gubaev K, Podryabinkin EV, et al. The mlip package: Moment tensor potentials with mpi and active learning. *Mach Learn Sci Technol* 2021;2:025002.
- [18] Hernandez A, Balasubramanian A, Yuan F, et al. Fast, accurate, and transferable many-body interatomic potentials by symbolic regression. *npj Comput Mater* 2019;5:112.
- [19] Drautz R. Atomic cluster expansion for accurate and transferable interatomic potentials. *Phys Rev B* 2019;99:014104.
- [20] Chen C, Ye W, Zuo Y, et al. Graph networks as a universal machine learning framework for molecules and crystals. *Chem Mater* 2019;31:3564–72.
- [21] Gasteiger J, Groß J, Günnemann S. Directional message passing for molecular graphs. arXiv:2003.03123, 2020.
- [22] Schütt KT, Sauceda HE, Kindermans PJ, et al. Schnet – a deep learning architecture for molecules and materials. *J Chem Phys* 2018;148:241722.
- [23] Xie T, Grossman JC. Crystal graph convolutional neural networks for an accurate and interpretable prediction of material properties. *Phys Rev Lett* 2018;120:145301.
- [24] Choudhary K, DeCost B. Atomistic line graph neural network for improved materials property predictions. *npj Comput Mater* 2021;7:185.
- [25] Chen C, Ong SP. A universal graph deep learning interatomic potential for the periodic table. *Nat Comput Sci* 2022;2:718–28.
- [26] Deng B, Zhong P, Jun K, et al. Chgnet as a pretrained universal neural network potential for charge-informed atomistic modelling. *Nat Mach Intell* 2023;5:1031–41.
- [27] Takamoto S, Shinagawa C, Motoki D, et al. Towards universal neural network potential for material discovery applicable to arbitrary combination of 45 elements. *Nat Commun* 2022;13:2991.
- [28] Choudhary K, DeCost B, Major L, et al. Unified graph neural network force-field for the periodic table: Solid state applications. *Digital Discovery* 2023;2:346–55.
- [29] Liang Y, Chen M, Wang Y, et al. A universal model for accurately predicting the formation energy of inorganic compounds. *Sci China Mater* 2023;66:343–51.
- [30] Merchant A, Batzner S, Schoenholz SS, et al. Scaling deep learning for materials discovery. *Nature* 2023;624:80–5.
- [31] Jain A, Ong SP, Hautier G, et al. Commentary: The materials project: A materials genome approach to accelerating materials innovation. *APL Mater* 2013;1.
- [32] Kirklin S, Saal JE, Meredig B, et al. The open quantum materials database (oqmd): Assessing the accuracy of dft formation energies. *npj Comput Mater* 2015;1:15010.
- [33] Dosovitskiy A, Beyer L, Kolesnikov A, et al. An image is worth 16x16 words: Transformers for image recognition at scale. arXiv: 2010.11929, 2020.
- [34] Devlin J, Chang M-W, Lee K, et al. Bert: Pre-training of deep bidirectional transformers for language understanding. arXiv:1810.04805, 2018.
- [35] Touvron H, Martin L, Stone K, et al. Llama 2: Open foundation and fine-tuned chat models. arXiv:2307.09288, 2023.
- [36] Vaswani A, Shazeer N, Parmar N, et al. Attention is all you need. arXiv:1706.03762, 2017.
- [37] Zhou J, Cui G, Hu S, et al. Graph neural networks: A review of methods and applications. *AI Open* 2020;1:57–81.
- [38] Wu Z, Pan S, Chen F, et al. A comprehensive survey on graph neural networks. *IEEE Trans Neural Networks Learn Syst* 2021;32:4–24.
- [39] Scarselli F, Gori M, Tsoi AC, et al. The graph neural network model. *IEEE Trans Neural Networks* 2009;20:61–80.

- [40] Paszke A, Gross S, Massa F, et al. Pytorch: An imperative style, high-performance deep learning library. arXiv:1912.01703, 2019.
- [41] Perdew JP, Burke K, Ernzerhof M. Generalized gradient approximation made simple. *Phys Rev Lett* 1996;77:3865–8.
- [42] Kresse G, Hafner J. Ab initio molecular dynamics for liquid metals. *Phys Rev B* 1993;47:558–61.
- [43] Kresse G, Hafner J. Norm-conserving and ultrasoft pseudopotentials for first-row and transition elements. *J Phys Condens Matter* 1994;6:8245.
- [44] Kresse G, Furthmüller J. Efficiency of ab-initio total energy calculations for metals and semiconductors using a plane-wave basis set. *Comput Mater Sci* 1996;6:15–50.
- [45] Kresse G, Furthmüller J. Efficient iterative schemes for ab initio total-energy calculations using a plane-wave basis set. *Phys Rev B* 1996;54:11169–86.
- [46] Loshchilov I, Hutter F. Decoupled weight decay regularization. arXiv:1711.05101, 2017.
- [47] Ying C, Cai T, Luo S, et al. Do transformers really perform bad for graph representation? arXiv: 2106.05234, 2021.
- [48] Liu L, Liu X, Gao J, et al. Understanding the difficulty of training transformers. arXiv: 2004.08249, 2020.
- [49] Yang JX, Zhao HL, Gong HR, et al. Proposed mechanism of hcp → fcc phase transition in titanium through first principles calculation and experiments. *Sci Rep* 1992;2018:8.
- [50] Bai F, Zhu Q, Shen J, et al. Study on phase transformation orientation relationship of hcp-fcc during rolling of high purity titanium. 2021;11:1164.
- [51] Baskes MJ, Johnson RA. Modified embedded atom potentials for hcp metals. *Model Simul Mater Sci Eng* 1994;2:147.
- [52] Kim Y-M, Lee B-J, Baskes MJ. Modified embedded-atom method interatomic potentials for ti and zr. *Phys Rev B* 2006;74:014101.
- [53] Zhang Z, Shao Y, Lotsch B, et al. New horizons for inorganic solid state ion conductors. *Energy Environ Sci* 2018;11:1945–76.
- [54] Qi J, Banerjee S, Zuo Y, et al. Bridging the gap between simulated and experimental ionic conductivities in lithium superionic conductors. *Mater Today Phys* 2021;21:100463.
- [55] Klimeš J, Bowler DR, Michaelides A. Chemical accuracy for the van der waals density functional. *J Phys Condens Matter* 2010;22:022201.
- [56] Asano T, Sakai A, Ouchi S, et al. Solid halide electrolytes with high lithium-ion conductivity for application in 4 v class bulk-type all-solid-state batteries. *Adv Mater* 2018;30:1803075.
- [57] Wang S, Liu Y, Mo Y. Frustration in super-ionic conductors unraveled by the density of atomistic states. *Angew Chem Int Edit* 2023;62:e202215544.
- [58] Liu Y, He X, Mo Y. Discrepancies and error evaluation metrics for machine learning interatomic potentials. *npj Comput Mater* 2023;9:174.
- [59] Liu Y, Mo Y. Assessing the accuracy of machine learning interatomic potentials in predicting the elemental orderings: A case study of li-al alloys. *Acta Mater* 2024;268:119742.



Fankai Xie is a Ph.D. candidate at Institute of Physics, Chinese Academy of Sciences. His research primarily focuses on machine learning force field, crystal property prediction and universal force field development.



Sheng Meng is a professor of physics at the Institute of Physics, Chinese Academy of Sciences. His research interest focuses on excited state quantum dynamics in condensed matters, energy conversion mechanism for sustainable society, as well as new algorithms and tools in materials computation.



Miao Liu is a professor at the Institute of Physics, Chinese Academy of Sciences. He is the leading founder of the atomly.net materials science database. His research revolves around data-driven materials science for energy materials, alloys, quantum materials, etc.